ChemElectroChem

Research Article
doi.org/10.1002/celc.202500344

Chemistry Europe
European Chemical Societies Publishing

www.chemelectrochem.org

# Insights into Electro-Oxidative Dehydrogenation of Aldehydes on Copper Foam: The Role of Electrode Design, Side Reactions, and Substrate Properties

Sonja D. Mürtz, Benni Zou, Simon Derichs, Justus Kümper, and Regina Palkovits*

A sustainable alternative to fossil-based energy sources is green hydrogen, which is produced by electrolysis, but the high energy demand of the oxygen evolution reaction (OER) limits its overall efficiency. Recent efforts aim to replace OER with low-potential anode reactions, such as the electro-oxidative dehydrogenation (EOD) of aldehydes, which simultaneously yield valuable chemical products. However, the mechanistic understanding of the EOD and the influence of catalyst structure and reaction conditions on selectivity and efficiency remain limited. Here, it is shown that the EOD of aldehydes on modified copper foam electrodes is strongly affected by electrode morphology, substrate concentration and structure, as well as electrolyte composition. It is demonstrated that increasing the electrochemically active surface area enhances current density up to a morphological diffusion limit reaching 110 mA $cm^{-2}$ at 0.3 V versus reversible hydrogen electrode (RHE). Higher furfural concentrations increase current density but simultaneously promote the non-faradaic Cannizzaro reaction, thereby reducing faradaic efficiency. Lower KOH concentrations partially suppress this side reaction, though 1 M remains optimal for EOD. Substrate screening reveals that electron-rich aldehydes impede the reaction, likely by hindering intermediate formation. The findings highlight the importance of the electrode morphology and the critical balance between substrate availability and parasitic side reactions in aldehyde EOD, offering practical guidelines for catalyst design and process optimization for low-potential hydrogen production.

## 1. Introduction

Green hydrogen is essential to transform today's linear-oriented chemical industry into a more sustainable one, producing less waste and $CO_2$ emissions.[1,2] To reduce the energy required for the formation of hydrogen via water electrolysis from renewable energies, one possibility is to find alternative anode reactions to the oxygen evolution reaction (OER).[3] These reactions can decrease the required potential below the thermodynamic minimum of the OER, while producing valuable products at the same time. Alcohols like methanol, ethanol, or glycerol offer advantageous products such as formic acid, acetic acid, or lactic acid with thermodynamic minimum potentials in the range of 0–0.1 V versus reversible hydrogen electrode (RHE). A lot of research has been done in this area in the past two decades, which led to promising results regarding selectivity. However, slow kinetics of these alcohol oxidation reactions cause potentials starting around 1 V versus RHE with current densities that rarely exceed 50 mA $cm^{-2}$.[4–8] More recently, Wang et al.[9] reported a low-potential aldehyde oxidation reaction as an alternative anode reaction. This approach promises to reduce the potential to around 0.3 V versus RHE at current densities up to 100 mA $cm^{-2}$, which would create a big benefit for the hydrogen production efficiency. In addition, the low-potential aldehyde oxidation, also called electro-oxidative dehydrogenation (EOD) of aldehydes, enables hydrogen atoms to recombine into $H_2$ at the anode, unlike conventional aldehyde electro-oxidation, where the hydrogen atoms are oxidized into $H_2O$ at higher potentials (see **Scheme 1**).

The EOD reaction is expected to proceed via geminal diolates, intermediates, which can be formed in alkaline media from aldehydes. The diolates facilitate at the same time the parasitic Cannizzaro disproportionation reaction: transforming two aldehydes into a carboxylate and an alcohol, thereby decreasing the efficiency of the electrochemical reaction.[10] Previous studies on formaldehyde oxidation on Au and Ag[11] and more recent data for acetaldehyde on Au[12] indicate that aldehyde oxidation reaches a mass transfer limitation with respect to total organic concentration even at less alkaline pH values. The concentration of the aldehyde greatly exceeds the diolate under these conditions, which indicates that the reaction may not require the

*S. D. Mürtz, B. Zou, S. Derichs, J. Kümper, R. Palkovits*
*Institute for Technical and Macromolecular Chemistry (ITMC)*
*RWTH Aachen University*
*Worringerweg 2, 52074 Aachen, Germany*
*E-mail: palkovits@itmc.rwth-aachen.de*

*R. Palkovits*
*Forschungszentrum Jülich GmbH*
*Institute for a Sustainable Hydrogen Economy (INW-2)*
*Marie-Curie Straße 5, 52428 Jülich, Germany*

*R. Palkovits*
*Max-Planck-Institute for Chemical Energy Conversion*
*Stiftstraße 34–26, 42470 Mülheim a.d. Ruhr, Germany*

*Supporting information for this article is available on the WWW under https://doi.org/10.1002/celc.202500344*

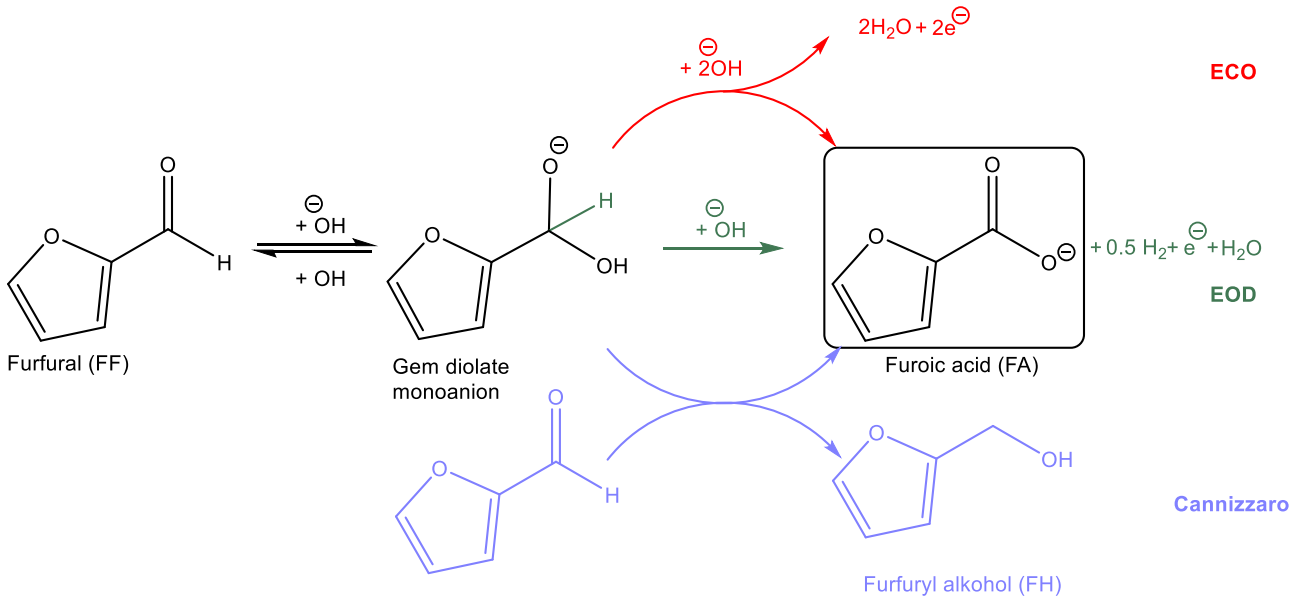


**Scheme 1.** Three reaction pathways of aldehydes in alkaline media: (red, top) Electrochemical oxidation (ECO) at high potentials (>1.0 V vs RHE) without $H_2$ evolution, (green, middle) EOD as the only $H_2$-generating route, and (blue, bottom) Cannizzaro as a base-driven non-faradaic disproportionation reaction.

solution-phase diolate on surfaces such as Au and Ag and that EOD can proceed under milder pH conditions than previously assumed. The underlying mechanism remains unclear.[10,12]

The bipolar hydrogen production system introduced by Wang et al.[9] involves 5-(hydroxymethyl)furfural and furfural (FF) oxidation on modified copper foams and is reported to use only 1/14 of the electricity input compared to conventional water electrolyzers. Besides copper, earlier cyclovoltammetric studies on formaldehyde oxidation, as well as a recent study by Ramos et al. on benzaldehyde oxidation indicate that Au and Ag could be used as catalysts for low-potential aldehyde oxidation.[11,13–17] To facilitate C–H activation, bimetallic combinations of Cu with Pd, Pt, and Ni have been investigated recently for furfural oxidation, demonstrating improved reaction rates and stability. The best-performing alloy was CuPt, reaching 498 mA $cm^{-2}$ at 0.6 V versus RHE.[18–21] Similar currents were reached in another recent study on formaldehyde oxidation on CuAg catalysts.[22] Furthermore, Fu et al. demonstrated that a $Cu_6Sn_5$ alloy sustains exceptionally high currents (915 mA $cm^{-2}$ at 0.4 V vs RHE) with a faradaic efficiency (FE) for $H_2$ approaching 200%, attributed to lowered C–H dehydrogenation barriers via alloying.[23] Yang et al. developed a self-reactivating Pd–Cu catalyst maintaining 400 mA $cm^{-2}$ at 0.42 V stably over 120 h, by continuously reducing oxidized Cu during operation.[3] These bimetallic systems not only enhance activity but also mitigate surface deactivation. Additional catalyst materials such as NiOOH,[24] silicon photoelectrodes,[25] substrates like glucose[26] and $\alpha$-H-alcohols,[27] and reactor configurations such as an acid-alkaline furfural hybrid battery[28] or a novel liquid flow fuel cell[29,30] were investigated.

However, advancements in EOD require further fundamental mechanistic insights and a comprehensive understanding of the role of the side reactions in order to improve the selectivity and stability of the system.[10]

In this study, the EOD of furfural as a model compound on modified Cu foams is investigated with focus on the effects of electrode modification, the Cannizzaro side reaction, as well as the substrate structure. The aim is to gain a deeper fundamental understanding of the catalyst material and the reaction conditions, thereby supporting future catalyst development and process optimization.

## 2. Results and Discussion

Our investigations are built upon the system published by Wang et al.[9] We adopted the reported procedure, including a wet-chemical oxidation method followed by calcination and electrochemical reduction to produce a metallic Cu foam catalyst with high electrochemically active surface area. Consistent with their results, the highest current density for the EOD of furfural of around 55 mA $cm^{-2}$ is reached in the forward scan of a cyclic voltammogram (CV) at around 0.5 V versus RHE (see Figure S1, Supporting Information).

### 2.1. Electrode Design

To gain more insights into the role of the reported Cu foam modification procedure, the characteristics of the electrode and their effect on the EOD of furfural were investigated. First, the double-layer capacity, which correlates with the electrochemically active surface area, was determined and systematically varied by adjusting the time of the oxidation step during electrode synthesis. **Figure 1** shows the double-layer capacity together with the current densities reached in batch electrolysis with 0.05 M furfural in 1 M KOH at 0.3 V versus RHE for different oxidation times. With an increasing oxidation time during Cu foam modification, the

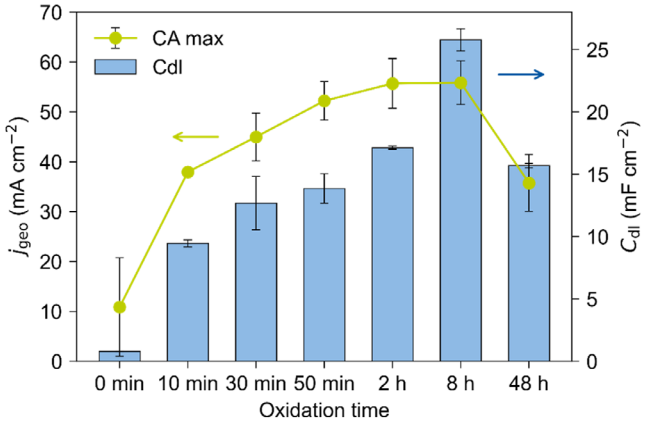


**Figure 1.** Maximum current density during electrolysis for electrodes prepared with different oxidation times and the corresponding electrode capacitance. Conditions: H-cell with Cu foam anode (WE, 1 cm$^2$) oxidized for 0–48 h, Hg/HgO (RE), graphite rod (CE); anolyte: 50 mM FF in 1 M KOH; stirring speed: 200 rpm; for chronoamperometric electrolysis experiments 0.3 V versus RHE was applied.

double layer capacity increases, which can be explained by the gradually growing micron needle structures observed with scanning electron microscopy (SEM) (Figure S2, Supporting Information). Prolonged oxidation times of 48 h, however, lead to a decrease in double-layer capacities by destroying the needle structure. The current density reaches a plateau at around 2 h of oxidation time, which might be due to morphological limitations such as restricted substrate access to active sites within the extended needle structures. Hence, diffusion limitation is likely for the reaction on the Cu foam modified with 8 h of oxidation.

Looking into the Nyquist plots of the electrodes reveals that the diameter of the half-circles, corresponding to the charge-transfer resistance, increases with longer oxidation times (**Figure 2**). This could be related to a thicker oxide layer that remains beneath the surface, thereby hindering charge transfer and increasing resistance. In addition, we observed a linear increase with a slope of around one at low frequencies for the catalyst that was oxidized for 8 h. This could indicate a Warburg-type impedance, which confirms the diffusion transfer limitation of this morphology (see Figure S2, Supporting Information).

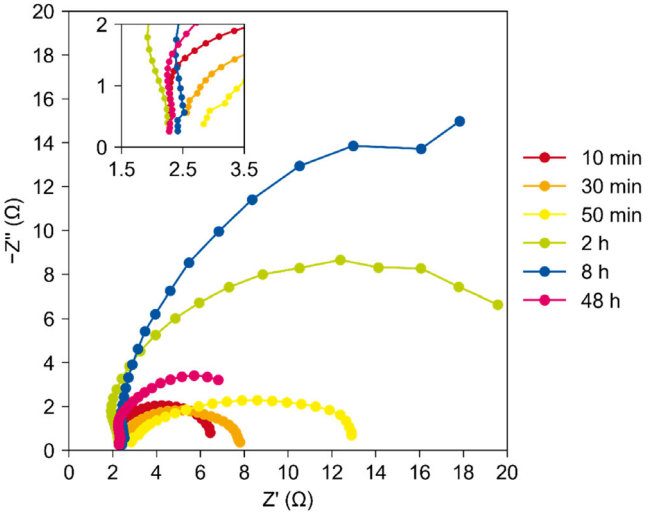


**Figure 2.** Nyquist plots resulting from impedance measurements of the electrodes prepared with different oxidation times. Conditions: H-cell with Cu foam anode (WE, 1 cm$^2$) oxidized for 0–48 h, Hg/HgO (RE), graphite rod (CE); anolyte: 50 mM FF in 1 M KOH; 0 rpm. EIS: 10 points dec$^{-1}$, $E_{ac}$ = 10 mV.

Moreover, a Janus-like structure was uncovered to form during the reported procedure present as visible color change from top to bottom, confirmed by SEM and x-ray diffraction (XRD) analysis (see Figure S3 to S5, Supporting Information). According to Gao et al.,[31] one possible explanation for the formation of the Janus structure during wet-chemical oxidative etching of copper foam electrodes in a stationary solution is the presence of a concentration gradient. Specifically, compared to the upper part of the solution, the $Cu^{2+}$ concentration at the bottom of the beaker is higher, facilitating its reaction with hydroxide ions to form $Cu(OH)_2$, while CuO is more likely to form on the upper surface. This might lead to a different morphology after reduction and higher activities in the EOD reaction of the bottom side of the electrode (see Figure S3b, Supporting Information). Hence, the bottom side was used for further investigations. Contact angle measurements showed that the surface hydrophilicity of the modified electrode is significantly enhanced compared to the blank, unmodified Cu foam (see Figure S6, Supporting Information). Overall, the modification procedure has a big influence on the electrode characteristics. Especially, the oxidation time changes the catalyst's morphology and double-layer capacity, which turned out to increase the current density of the reaction up to a plateau, likely due to diffusion limitations.

To increase mass transport within the system, the stirring speed was investigated for the Cu foams modified with 2 and 8 h of oxidation time, as depicted in **Figure 3**. As expected, higher stirrings of up to 500 rpm increase the current density in CV measurements to over 100 mA cm$^{-2}$. However, further increasing the stirring speed to 800 rpm does not further improve the current density due to the formation of a vortex, decreasing the active electrode area. This proves that diffusion limitations play a vital

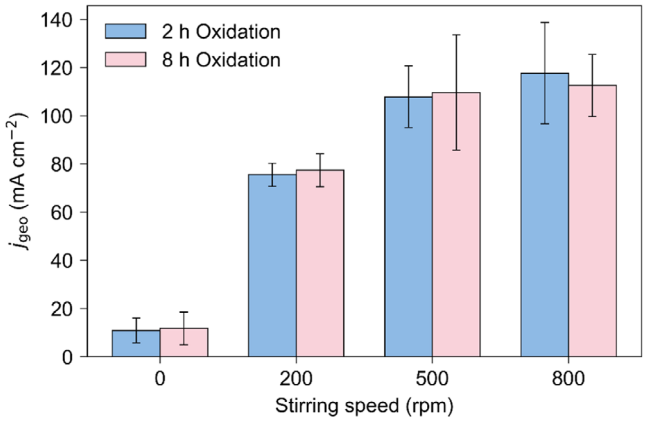


**Figure 3.** Effect of different stirring speeds on maximum current density in CVs. Conditions: H-cell with a modified Cu foam anode (WE, 1 cm$^2$) oxidized for 2 or 8 h, Hg/HgO (RE), graphite rod (CE); anolyte: 50 mM FF in 1 M KOH; stirring speed: 0–800 rpm; CV potential window: 0–0.6 V versus RHE with a scan rate of 0.005 V s$^{-1}$.

role in the system. However, the electrodes with oxidation times of 2 and 8 h result in similar current densities for all stirring speeds. Hence, the maximum current density is also structurally limited and cannot be further increased by stirring speed.

In addition to electrode morphology and stirring speed, the substrate concentration might also influence adsorption capacity and reaction rate. However, as described above, increased substrate concentrations might also increase the second-order Cannizzaro reaction.

### 2.2. Cannizzaro side reaction

The Cu foam electrode prepared with an oxidation time of 2 h was chosen for further electrolysis. The conversion and product yields of the chronoamperometric electrolysis at 0.3 V versus RHE after 0.3 Faraday equivalents ($F_{eq}$) are depicted on the left in **Figure 4**. Furoic acid (FA) is the main product, and the FE seems to be close to 100%, as reported in literature.[9] However, furfuryl alcohol (FH) was also detected after electrolysis, originating from the non-faradaic Cannizzaro reaction together with FA. On the right in Figure 4, the product spectrum of the reference experiment under the same conditions but without a potential is shown, indicating the occurring non-faradaic reactions. FA (10(±1)%) and FH (9(±1)%) are produced in a 1:1 ratio, which proofs the Cannizzaro pathway. As mentioned in literature,[9] this non-faradaic side reaction might be suppressed by applying a potential but the presence of FH after electrolysis indicates that it is still present under electrolysis conditions. To determine the real FE (darker pink), the amount of faradaic FA is calculated as the amount of produced FA (top of the bar) subtracted by the amount of FH (brighter portion) present. Therefore, the top of the dark green bar on the left in Figure 4 is the yield of FA produced in EOD. This is based on the assumption that FH is not further oxidized under electrolysis conditions, which was shown in reference experiments (Figure S7, Supporting Information). The real FE to FA is then close to 100%.

The Cannizzaro reaction is a second-order reaction since two furfural molecules react to FA and FH, while the EOD reaction is a first-order reaction, as shown in Scheme 1. Hence, decreasing the concentration could improve the FE by suppressing the non-faradaic side reaction. **Figure 5** shows the maximum current density reached in electrolysis with different furfural concentrations. Lower concentrations lead to lower current densities, while a plateau of around 110 mA cm$^{-2}$ is reached above 100 mM furfural. This might be due to less substrate–electrode interaction for lower concentrations, while non-faradaic side reactions become increasingly competitive at higher concentrations.

This can be proven by looking at the product ratios. They are calculated as normalized selectivities based solely on FF, FA, and FH resulting from electrolysis and Cannizzaro reaction, excluding the missing mass of 5–10% attributed to humin formation[32] (details in SI). The results of the reference reaction (**Figure 6**, right) show that around one third of the FF undergoes the Cannizzaro reaction at FF concentration of 200 mM. Reducing the concentration to 10 mM almost fully suppresses this reaction. In comparison, the product ratios for the electrolysis at 0.3 $F_{eq}$ follow the same trend, resulting in significant amounts of FH from the non-faradaic reaction at 100 and 200 mM FF, respectively. Hence, we observe a trade-off between low furfural concentrations that hinder the Cannizzaro reaction and higher concentrations that lead to higher current densities.

Another parameter that could influence the ratio between the faradaic EOD and non-faradaic side reactions could be the OH$^-$ concentration. A recent study on acetaldehyde oxidation reported a mass transfer limitation with respect to total organic concentration over a wide pH range. In mild alkaline conditions, the concentration of the aldehyde greatly exceeds the diolate, which indicates that the EOD reaction might not require the diolates as an intermediate.[10,12] Hence, lowering the pH could

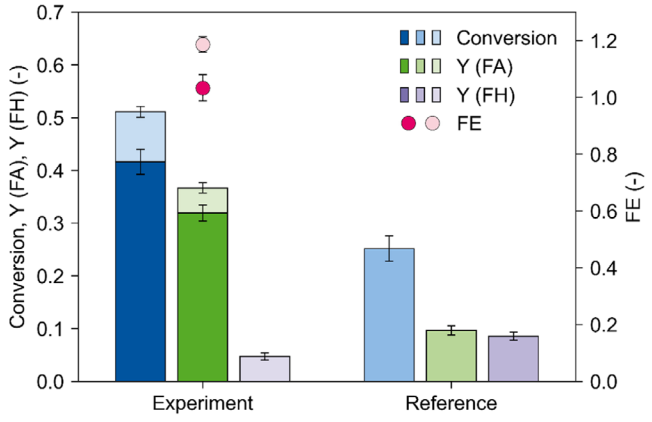


**Figure 4.** Conversion, yields, and FE based on HPLC analysis after electrolysis and a reference experiment without applying a potential. Cannizzaro products are shown in brighter colors, and darker colors therefore represent the corrected values for the EOD reaction. Conditions: H-cell with Cu foam anode (WE, 1 cm$^2$) oxidized for 2 h, Hg/HgO (RE), graphite rod (CE), anolyte: 50 mM FF in 1 M KOH; stirring speed: 500 rpm; electrolysis and reference experiments were performed for the same duration. For electrolysis experiments: 0.3 V versus RHE was applied up to 0.3 $F_{eq}$.

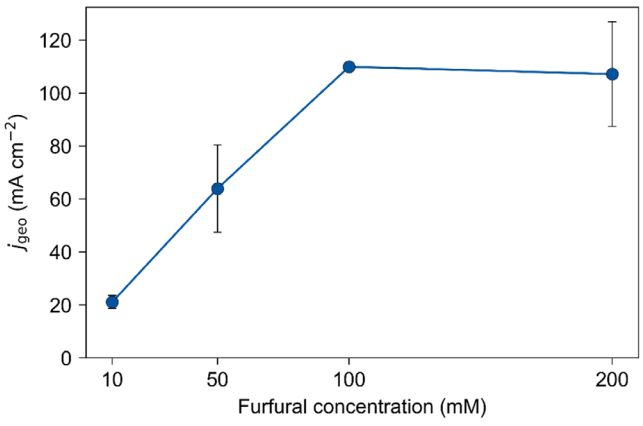


**Figure 5.** Maximum current density of chronoamperometry (CA) electrolysis with different FF concentrations. Conditions: H-cell with Cu foam anode (WE, 1 cm$^2$) oxidized for 2 h, Hg/HgO (RE), graphite rod (CE); anolyte: 10–200 mM FF in 1 M KOH; stirring speed: 500 rpm; electrolysis and reference experiments were performed for the same duration. For electrolysis experiments: 0.3 V versus RHE, 0.3 $F_{eq}$.

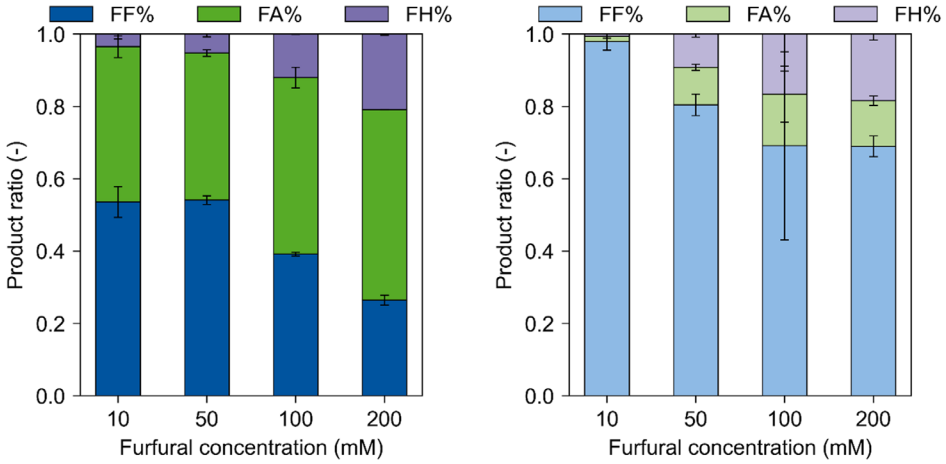


**Figure 6.** Normalized substrate ratio after CA electrolysis (left) and reference experiment without applying a potential (right) for different FF concentrations (Calculation details in SI, part 3). Conditions: H-cell with Cu foam anode (WE, 1 $cm^2$) oxidized for 2 h, Hg/HgO (RE), graphite rod (CE); anolyte: 10–200 mM FF in 1 M KOH; stirring speed: 500 rpm. Duration time for electrolysis and reference experiment are equal. For electrolysis experiments: 0.3 V versus RHE, 0.3 $F_{eq}$.

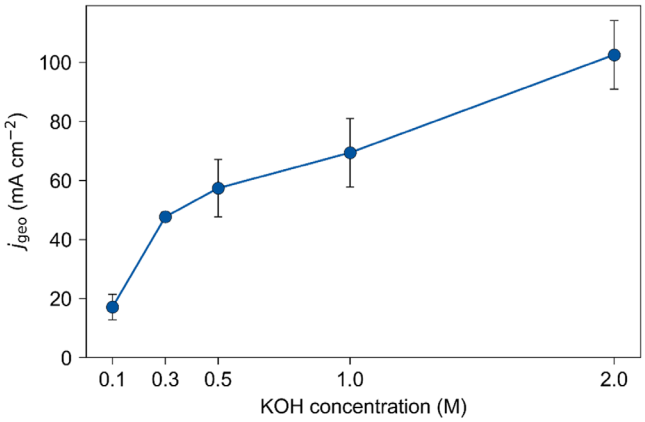


**Figure 7.** Maximum current density of CA electrolysis with different KOH concentrations. Conditions: H-cell with Cu foam anode (WE, 1 $cm^2$) oxidized for 2 h, Hg/HgO (RE), graphite rod (CE); anolyte: 50 mM FF in 0.1–2 M KOH; stirring speed: 500 rpm. For electrolysis experiments 0.3 V versus RHE, 0.3 $F_{eq}$.

decrease the diolate formation, which may suppress the Cannizzaro reaction that proceeds via this intermediate.

**Figure 7** shows that in chronoamperometric measurements using electrolytes with varying KOH concentrations, the maximum current density increases continuously with rising KOH concentration from 0.1 to 2 M. Notably, a steep increase in current density is observed between 0.1 and 0.5 M, while the rate of increase slows down above 0.5 M. This behavior may be related to a higher activity of the diolate which is the dominant species at higher pH values and KOH concentrations.

Lower KOH concentrations in the reference experiments under the same conditions without applying a potential decrease the Cannizzaro reaction from 19(±2)% to 9(±1)% conversion when reducing the KOH concentration from 2 to 0.3 M (see **Figure 8**, right). This decrease is less pronounced for the electrolysis experiments (Figure 8, left), where it is significant from 14(±2)% to 6(±1)% with regard to formed FH when decreasing

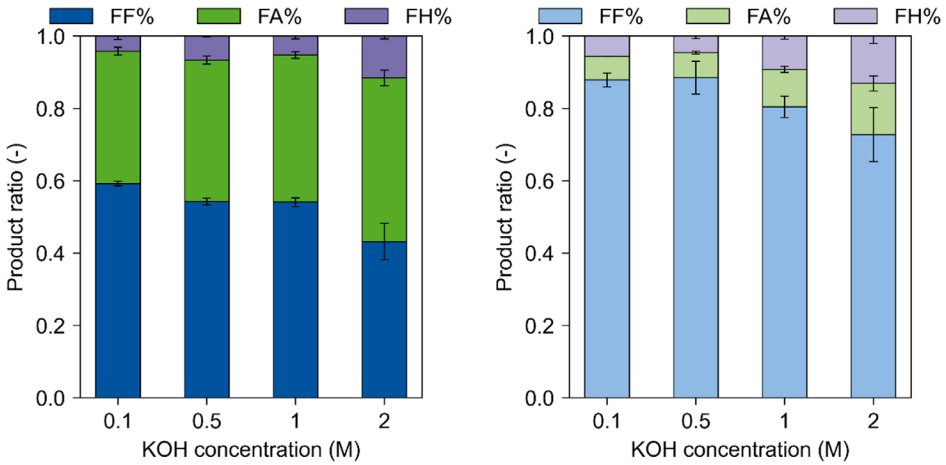


**Figure 8.** Normalized substrate ratio after CA electrolysis (left) and reference experiment without applying a potential (right) for different KOH concentrations (Calculation details in SI, part 3). Conditions: H-cell with Cu foam anode (WE, 1 $cm^2$) oxidized for 2 h, Hg/HgO (RE), graphite rod (CE); anolyte: 0.3–2 M FF in KOH; stirring speed: 500 rpm. Duration time for electrolysis and reference experiment are equal. For electrolysis experiments: 0.3 V versus RHE, 0.3 $F_{eq}$.

the KOH concentration from 2 to 1 M. Overall, lower substrate concentrations suppress the Cannizzaro reaction more strongly than lower KOH concentrations.

### 2.3. Substrate Properties

Furfural is a model compound and represents one specific bio-based aldehyde. To transfer the gained knowledge and system to other substrates, it is important to understand how structural properties of the substrate influence the reaction. Therefore, different compounds with structure modifications relative to furfural were tested. First, the oxygen in the ring was replaced with sulfur (thiophene-2-carbaldehyde) and with nitrogen (pyrrol-2-carboxaldehyde), which decreases the electron-withdrawing effect of the ring. As depicted in **Figure 9**, the current density of the EOD of furfural derivatives decreased with lower electronegativity of the heteroatom. In addition, benzaldehyde and its methoxy-/hydroxy-derivatives were investigated. The current density is decreasing with the addition of methoxy groups. The position of the methoxy groups also influences the current in a decreasing manner, following the trend ortho > para > meta. Substitution with a hydroxy group has an even higher impact and results in the lowest observed current density. Methoxy groups possess a positive mesomeric effect, donating electron-density into the aromatic ring, which might increase the electron density at the carbonyl group, similar to sulfur and nitrogen in the heterocyclic compounds. This mesomeric effect is even stronger for hydroxy groups, which is consistent with the trend depicted in Figure 9. Substrates, such as cyanofurfural and nitrobenzaldehyde, bearing electron-withdrawing substituents, were tested but could not be measured because of decomposition and polymerization under the reaction conditions. Hence, it can be concluded that an increased electron density at the carbonyl group decreases the current density and thus causes a slower EOD reaction rate. This behavior could be related to the stability of the diolate intermediate or its formation, which could be favored by decreasing the electron density at the carbonyl group.

### 2.4. Long-Term Stability in Flow Cell

Investigating the long-term catalytic stability of the electrode in a circular flow-cell system based on FF as substrate provides insights into electrode reusability and redirects the focus back to the electrode material. As the conversion increased, the concentration of unreacted FF gradually decreased, leading to a continuous decline in current density, which slowed down in the later stage of electrolysis. When charge for a theoretical conversion of ≈80% was transferred, the anolyte was replaced with a fresh FF solution to sustain the electrolysis in a new run. The chronoamperometry (CA) curve of the first run is shown in **Figure 10** (left), while the corresponding conversion, yield, and FE calculated from high-performance liquid chromatography (HPLC) analysis are presented in Figure 10 (right). The results show that both conversion and FA yield continuously increase, with only trace amounts of FH detected, comparable to the batch experiments. The discrepancy between conversion and yield may be attributed to increased side reactions, such as humin formation, related to the longer reaction times. Current density dropped from around 100 mA $cm^{-2}$ in batch to only around 10 mA $cm^{-2}$ under flow conditions. This is related to slow flow rates of up to 20 mL $min^{-1}$ of this setup, limiting the mass transport, and should be optimized in further studies.

The electrode was further tested for six consecutive cycles, and the continuous CA curves are shown in Figure S9. At the beginning of every cycle, the current density returned to around 10 mA $cm^{-2}$, indicating a high long-term stability of the electrode over ≈7.5 h of operation. The corresponding HPLC-derived results for each cycle are summarized in Figure S10, Supporting Information. The FE decreased from 80% in the first cycle to 60% in the last cycle. This degradation is likely associated with surface aggregation and structural densification of the catalyst upon extended operation. The resulting reduction of active sites, elongation of charge-transfer pathways, and increase in interfacial resistance collectively hinder electron and mass transport, thereby lowering the overall FE.

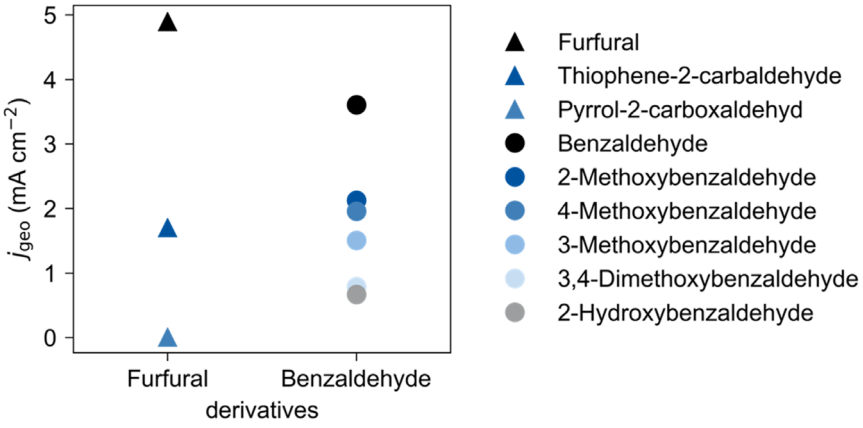


**Figure 9.** Comparison of maximum current density in CVs of different types of furfural and benzaldehyde derivatives (structures in Figure S8). Conditions: H-cell with modified Cu foam (WE, 1 $cm^2$) oxidized for 2 h, Hg/HgO (RE), glassy carbon (CE); anolyte: 50 mM aldehyde derivatives in 0.1 M KOH aqueous solution with 20 vol% ACN; stirring speed: 0 rpm. CV potential window: 0–0.53 V versus RHE with a scan rate of 0.01 V $s^{-1}$.

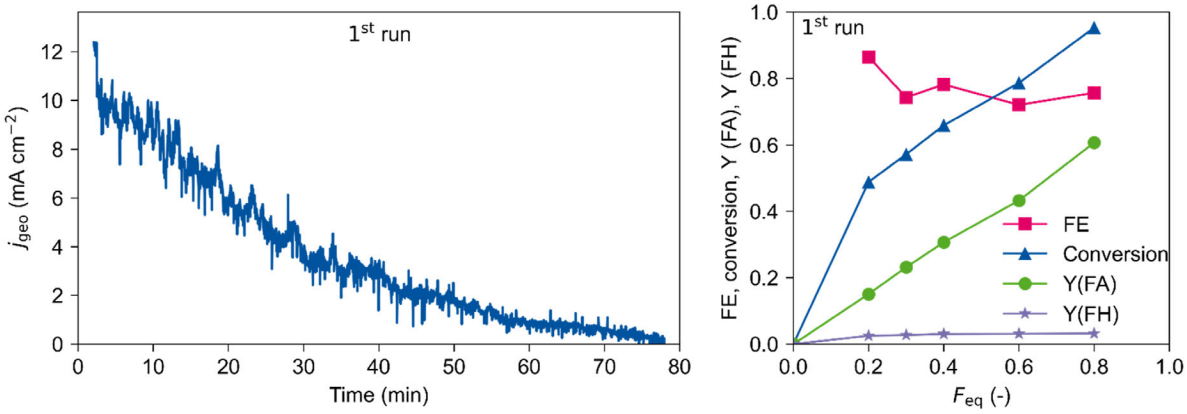


**Figure 10.** CA curves of the catalyst in a circular flow cell (left) and the corresponding conversion, yield, and FE calculated from HPLC analysis of the electrolyte (right). Conditions: Flow cell with modified Cu foam (WE, 25 cm$^2$) oxidized for 2 h, Hg/HgO (RE), carbon paper (CE); anolyte: 50 mM furfural in 0.1 M KOH, 0.3 V versus RHE.

## 3. Conclusion

In this study, the EOD of furfural was investigated as a low-potential alternative anode reaction for green hydrogen production. Modified Cu foam electrodes were synthesized via a wet-chemical oxidation process, reported by Wang et al.[9] The dependence of catalytic performance on oxidation time during the electrode synthesis, which directly influenced the morphology, electrochemically active surface area, and charge-transfer resistance, was systematically investigated. While increased surface area by longer oxidation times resulted in improved current densities, diffusion limitations and internal resistances limited the current to around 110 mA cm$^{-2}$ in batch electrolysis at 0.3 V versus RHE at Cu foam electrodes with oxidation times of 2 h. The presence and impact of the non-faradaic Cannizzaro side reaction were evaluated under varying furfural (FF) and KOH concentrations. Results have shown that high FF concentrations increased current density but also promoted Cannizzaro byproduct formation, which reduces the FE, resulting in a trade-off between achieving high reaction rates and maintaining high FEs. In addition, the Cannizzaro reaction could be mildly suppressed by lowering KOH concentrations. Hence, decreasing the concentration of the diolate slows down the non-faradaic reaction more than the faradaic EOD reaction. The effects of the substrate structure on the current density were investigated. Electron-donating groups such as methoxy and hydroxy substituents hindered the reaction, likely due to reduced formation or stability of the proposed diolate intermediate, while electron-withdrawing groups, lowering electron densities at the carbonyl group, could potentially promote EOD. Lastly, the stability of the Cu anode was shown in long-term flow experiments. Overall, the study provides fundamental insights into catalyst design, operating conditions, and substrate effects for the EOD of aldehydes. These findings support future catalyst development and process optimization for low-potential anode reactions for energy-efficient electrochemical hydrogen production processes.

## 4. Experimental Section

### Synthesis of the Modified Cu Foams

Cu foam electrodes were prepared via a three-step process involving wet-chemical oxidation, thermal reduction, and electrochemical reduction. First, Cu foam was ultrasonically cleaned in 2 M HCl for 5 min, followed by sequential ultrasonic cleaning in ethanol and deionized water (5 min each). The cleaned foam was then immersed in an aqueous oxidizing solution containing 2.67 M NaOH and 0.13 M $(NH_4)_2S_2O_8$ for varying durations (10, 30, 50 min, 2 , 8 , and 48 h). After oxidation, the electrode was washed with deionized water and dried overnight (16 h) at 60 °C. Subsequently, the oxidized samples were thermally calcined in a tube furnace at 550 °C for 3 h under constant nitrogen flow, with a ramp rate of 1 °C min$^{-1}$. Finally, the electrodes were reduced at −0.4 V versus RHE for 400 s in 1 M KOH prior to use.

### Electrolysis Experiments

CVs were recorded in a H-type cell using a Hg/HgO and a graphite rod reference electrode (glassy carbon for substrate screening) as counter electrode. The working electrode was copper foam with oxidation time from 10 min to 48 h. The anolyte consisted of KOH solution (0.3–2 M) and furfural (10–200 mM). The catholyte was pure KOH solution with identical KOH concentration but without furfural. To separate the anode and cathode chambers, a Nafion N-324 membrane was employed. During reactions nitrogen was purged through the anode compartment to remove dissolved oxygen. CV measurements were performed in the range of 0–0.53 V versus RHE with a scan rate of 0.005 V s$^{-1}$ and a step size of 0.00244 V. Electrolysis was carried out at 0.3 V versus RHE constant potentials at room temperature. Reaction mixtures were analyzed by HPLC (Shimadzu Prominence LC-20 system) to quantify furfural and oxidation products.

### Long-Term Testing Experiments

A Flex-E-Cell system (FXC Engineering GmbH) was used for the three-electrode flow electrolysis experiments. The working electrode (WE) was a Cu foam anode (5 × 5 cm$^2$) oxidized for 2 h, while a carbon paper of the same size served as the counter electrode (CE). A

Hg/HgO (1 M KOH) electrode was used as the reference electrode (RE). The anode and cathode compartments were separated by a Nafion membrane. The anolyte consisted of 50 mM furfural dissolved in 100 mL of 1 M KOH aqueous solution, and the catholyte was 100 mL of 1 M KOH. The flow rates of both anolyte and catholyte were maintained at 20 mL $min^{-1}$.[33–36]

## Supporting Information

The authors have cited additional references within the Supporting Information.[34,35,36,37]

## Acknowledgements

S.D.M. and B.Z. contributed equally to this work. The authors would like to thank Jens Heller for the HPLC analysis and Noah Avraham-Radermacher for XRD analysis. Financial support from the Federal Ministry of Research, Technology and Space (BMFTR) within the project (ID: 03SF0727A) Hydrogen4Tomorrow is gratefully acknowledged. This work was also supported by the Cluster of Excellence Fuel Science Center (EXC 2186, ID: 390919832) funded by the Excellence Initiative by the German federal and state governments to promote science and research at German universities. The authors acknowledge the funding by the German Federal Ministry of Research, Technology and Space (BMFTR) and the Ministry of Economic Affairs, Industry, Climate Action and Energy of the State of North Rhine-Westphalia through the project HC-H2.

Open Access funding enabled and organized by Projekt DEAL.

## Conflict of Interest

The authors declare no conflicts of interest.

## Data Availability Statement

The data that support the findings of this study are available via Zenodo: DOI: 10.5281/zenodo.17631132.

**Keywords:** cannizzaro reaction · copper foam electrodes · electro-oxidative dehydrogenation · furfural oxidation · green hydrogen production

[1] P. Gabrielli, L. Rosa, M. Gazzani, R. Meys, A. Bardow, M. Mazzotti, G. Sansavini, *One Earth* **2023**, *6*, 682.
[2] S. van Renssen, *Nat. Clim. Change* **2020**, *10*, 799.
[3] D. Yan, C. Mebrahtu, S. Wang, R. Palkovits, *Angew. Chem. Int. Ed.* **2023**, *62*, e202214333.
[4] Y. Tong, X. Yan, J. Liang, S. X. Dou, *Small* **2021**, *17*, 1904126.
[5] C. Li, K. Wang, D. Xie, *Surf. Interfaces* **2022**, *28*, 101594.
[6] P. A. Alaba, C. S. Lee, F. Abnisa, M. K. Aroua, P. Cognet, Y. Pérès, W. M. A. W. Daud, *Rev. Chem. Eng.* **2021**, *37*, 779.
[7] S. D. Mürtz, F. Musialek, N. Pfänder, R. Palkovits, *ChemElectroChem* **2023**, e202201114.
[8] L. Fei, H. Sun, Y. Li, Y. Gu, W. Zhou, Z. Shao, *Energy Environ. Sci.* **2025**, *18*, 6456.
[9] T. Wang, L. Tao, X. Zhu, C. Chen, W. Chen, S. Du, Y. Zhou, B. Zhou, D. Wang, C. Xie, P. Long, W. Li, Y. Wang, R. Chen, Y. Zou, X.-Z. Fu, Y. Li, X. Duan, S. Wang, *Nat. Catal.* **2021**, *5*, 66.
[10] N. C. Ramos, A. Holewinski, *Curr. Opin. Electrochem.* **2024**, *45*, 101484.
[11] M. Bełtowska-Brzezinska, *Electrochim. Acta* **1985**, *30*, 1193.
[12] C. J. Bondue, M. Spallek, L. Sobota, K. Tschulik, *ChemSusChem* **2023**, *16*, e202300685.
[13] N. A. Anastasijevic, H. Baltruschat, J. Heitbaum, *Electrochim. Acta* **1993**, *38*, 1067.
[14] Z. Jusys, *J. Electroanal. Chem.* **1994**, *375*, 257.
[15] Z. Jusys, A. Vaškelis, *J. Electroanal. Chem.* **1992**, *335*, 93.
[16] M. V. ten Kortenaar, Z. I. Kolar, J. J. M. de Goeij, G. Frens, *J. Electrochem. Soc.* **2001**, *148*, E327.
[17] N. C. Ramos, H. Neyer, J. W. Medlin, A. Holewinski, *J. Electrochem. Soc.* **2024**, *171*, 126507.
[18] H. Liu, N. Agrawal, A. Ganguly, Y. Chen, J. Lee, J. Yu, W. Huang, M. M. Wright, M. J. Janik, W. Li, *Energy Environ. Sci.* **2022**, *15*, 4175.
[19] H. Liu, J. Yu, Y. Chen, J. Lee, W. Huang, W. Li, *ACS Appl. Mater. Interfaces* **2023**, *15*, 37477.
[20] X. Zhang, T.-Y. Liu, Y. Zhou, L. Zhang, X.-C. Zhou, J.-J. Feng, A.-J. Wang, *Appl. Catal. B Environ.* **2023**, *328*, 122530.
[21] M. Yang, Y. Jiang, C.-L. Dong, L. Xu, Y. Huang, S. Leng, Y. Wu, Y. Luo, W. Chen, T. T. T. Nga, S. Wang, Y. Zou, *Nat. Commun.* **2024**, *15*, 9852.
[22] G. Li, G. Han, L. Wang, X. Cui, N. K. Moehring, P. R. Kidambi, D. Jiang, Y. Sun, *Nat. Commun.* **2023**, *14*, 525.
[23] X. Fu, D. Cheng, A. Zhang, J. Zhou, S. Wang, C. Wan, X. Zhao, J. Chen, P. Sautet, Y. Huang, X. Duan, *Angew. Chem. Int. Ed Engl.* **2025**, *64*, e202503828.
[24] J. Woo, B. C. Moon, U. Lee, H.-S. Oh, K. H. Chae, Y. Jun, B. K. Min, D. K. Lee, *ACS Catal.* **2022**, *12*, 4078.
[25] M. Ko, M. Lee, T. Kim, W. Jin, W. Jang, S. W. Hwang, H. Kim, J. H. Kwak, S. Cho, K. Seo, J.-W. Jang, *Nat. Commun.* **2025**, *16*, 2701.
[26] T. Faverge, B. Gilles, A. Bonnefont, F. Maillard, C. Coutanceau, M. Chatenet, *ACS Catal.* **2023**, *13*, 2657.
[27] D. Si, M. Wang, X. Yang, C. Wang, K. Shi, B. Huang, L. Chen, J. Shi, *Appl. Catal. B Environ.* **2023**, *331*, 122664.
[28] X. Zhang, W. Zhu, H. Zhou, L. Sun, Z. Wang, H. Liang, *Chem. Commun.* **2023**, *59*, 6837.
[29] D. Ouyang, D. Gao, J. Hong, Z. Jiang, X. Zhao, *J. Energy Chem.* **2023**, *79*, 135.
[30] T. Wang, Z. Huang, T. Liu, L. Tao, J. Tian, K. Gu, X. Wei, P. Zhou, L. Gan, S. Du, Y. Zou, R. Chen, Y. Li, X.-Z. Fu, S. Wang, *Angew. Chem. Int. Ed.* **2022**, *61*, e202115636.
[31] D. Gao, S. Liu, R. Liu, C. Streb, *Chem.—Eur. J* **2020**, *26*, 11109.
[32] B. Chen, Q. Hou, R. L. Smith, X. Qi, H. Guo, *Green Chem.* **2025**, *27*, 8414.
[33] H. R.Oswald, A. Reller, H. W. Schmalle, E. Dubler, *Acta Cryst.* **1990**, *46*, 2279.
[34] S. Asbrink, L. J.Norrby, *Acta Cryst.* **1970**, *26*, 8.
[35] R. Restori, D. Schwarzenbach, *Acta Cryst.* **1986**, *42*, 201.
[36] E. G. Shkvarina, A. A. Titov, A. S. Shkvarin, J. R. Plaisier, L. Gigli, A. N. Titov, *Acta Cryst.* **2018**, *74*, 1020.

Manuscript received: August 31, 2025
Revised manuscript received: October 29, 2025
Version of record online: